



HAL
open science

Experimental and numerical investigation of two-phase pressure drop in vertical cross-flow over a horizontal tube bundle

Khalid Bamardouf, David A Mcneil

► **To cite this version:**

Khalid Bamardouf, David A Mcneil. Experimental and numerical investigation of two-phase pressure drop in vertical cross-flow over a horizontal tube bundle. Applied Thermal Engineering, 2009, 29 (7), pp.1356. 10.1016/j.applthermaleng.2008.04.011 . hal-00537675

HAL Id: hal-00537675

<https://hal.science/hal-00537675>

Submitted on 19 Nov 2010

HAL is a multi-disciplinary open access archive for the deposit and dissemination of scientific research documents, whether they are published or not. The documents may come from teaching and research institutions in France or abroad, or from public or private research centers.

L'archive ouverte pluridisciplinaire **HAL**, est destinée au dépôt et à la diffusion de documents scientifiques de niveau recherche, publiés ou non, émanant des établissements d'enseignement et de recherche français ou étrangers, des laboratoires publics ou privés.

Accepted Manuscript

Experimental and numerical investigation of two-phase pressure drop in vertical cross-flow over a horizontal tube bundle

Khalid Bamardouf, David A McNeil

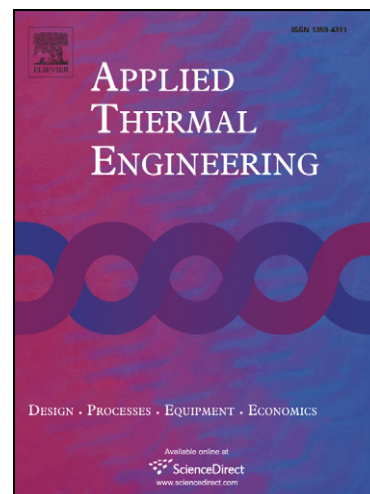
PII: S1359-4311(08)00200-7
DOI: [10.1016/j.applthermaleng.2008.04.011](https://doi.org/10.1016/j.applthermaleng.2008.04.011)
Reference: ATE 2486

To appear in: *Applied Thermal Engineering*

Received Date: 5 November 2007
Revised Date: 10 April 2008
Accepted Date: 10 April 2008

Please cite this article as: K. Bamardouf, D.A. McNeil, Experimental and numerical investigation of two-phase pressure drop in vertical cross-flow over a horizontal tube bundle, *Applied Thermal Engineering* (2008), doi: [10.1016/j.applthermaleng.2008.04.011](https://doi.org/10.1016/j.applthermaleng.2008.04.011)

This is a PDF file of an unedited manuscript that has been accepted for publication. As a service to our customers we are providing this early version of the manuscript. The manuscript will undergo copyediting, typesetting, and review of the resulting proof before it is published in its final form. Please note that during the production process errors may be discovered which could affect the content, and all legal disclaimers that apply to the journal pertain.



Experimental and numerical investigation of two-phase pressure drop in vertical cross-flow over a horizontal tube bundle

Khalid Bamardouf and David A McNeil *

Department of Mechanical Engineering, Heriot-Watt University, Riccarton, Edinburgh UK EH14 4AS,

*e-mail: D.A.McNeil@hw.ac.uk

Abstract

Experimental pressure-drop data for vertical two-phase air-water flow across horizontal tubes is presented for gas mass fractions in the range 0.0005-0.6 and mass fluxes in the range 25-700 kg/m²s. The square in-line tube bundle had one column containing ten tubes and two columns of half tubes attached to the walls. The tubes had a diameter of 38 mm and a pitch to diameter ratio of 1.32. This data and air-water and R113 vapour-liquid data available in the literature are compared with the predictions from two kettle reboiler models, the one-dimensional model and a one-dimensional formulation of the two-fluid model. The one-dimensional model was implemented with three separate void fraction correlations and one two-phase friction multiplier correlation. The results show that the two-fluid model predicts air-water void fraction data well but R113 data poorly with pressure drop predictions for both being unsatisfactory. The one-dimensional model is shown to predict pressure-drop and void fraction data reasonably well, provided a careful choice is made for the void fraction correlation.

Keywords: kettles, re-boilers, two-phase, two-dimensional, pressure-drop

1 Introduction

Shell and tube heat exchangers are widely used in the process industry with the kettle reboiler being one of the most common. A kettle reboiler consists of a tube bundle placed in a shell. The heating fluid flows inside the tubes while the heated fluid boils outside the tubes, figure 1. The difference in densities between the two-phase mixture flowing in the bundle and the liquid flowing between the bundle and the shell wall causes natural circulation to occur. To determine the circulation flow rate, different modelling approaches have been proposed.

The simplest approach is the one-dimensional model, where the liquid is assumed to enter the bundle from the bottom and evaporate while it moves vertically upwards. The two-phase pressure drop in the tube bundle is assumed equal to the static head of the liquid between the bundle and the shell. Since the two-phase pressure drop has gravity, acceleration and friction components, the void fraction and a two-phase friction multiplier are required to complete the model. Several investigators have proposed void fraction correlations, e.g. Schrage et al. [1], Dowlati et al. [2] and Feenstra et al. [3]. For the two-phase multiplier, various investigators have applied the Lockhart and Martinelli [4] method, represented by a simple correlation designed by Chisholm and Laird [5]. The one-dimensional model provides satisfactory prediction at low heat flux. However, at heat fluxes greater than 20 kW/m^2 , the flow becomes two-dimensional, Burnside et al. [6].

Attempts to model the two-dimensional flow have been made using the algebraic slip model and the two-fluid model. The former assumes that the two phases move in the same direction but with different velocities and was used by Burnside [7]. The two-fluid model is a more advanced approach to modelling the two-phase flow in a complex geometry. The model assumes that each phase has its own conservation equations describing mass, momentum and energy. These are solved together with closure equations used to define the interaction between the phases and between the phases and the tubes in the bundle. The interfacial drag coefficient allows the drag force between the phases to be found and is one of the most important closure equations because it strongly affects the void fraction and consequently influences the pressure drop.

Edwards and Jensen [8] produced a 2-D model for the kettle reboiler using the two-fluid approach. However, due to the absence of information on the interfacial momentum force at that time, the authors assumed a constant drag coefficient for the whole flow field. The value used allowed the experimental void fraction results to be approached, but convergence problems appeared when they got within 30% of the experimental values.

Rahman et al. [9] were the first to model the interfacial drag coefficient for vertical two-phase flow across a horizontal tube bundle. The drag coefficient was developed from experimental data with the assumption of negligible resistance between the tube walls and the gas or vapour flow, arguing that only the liquid phase was in contact with the tubes in the bundle. The drag coefficient was correlated as a power law function of the Reynolds number.

Stosic and Stevanovic [10], Stevanovic et al. [11], Stevanovic et al. [12] and Pezo et al. [13] proposed two correlations for the drag coefficient, one for the bubbly flow regime and the other for the churn flow regime. They derived their coefficients from the air-water void fraction measurements reported by Dowlati et al. [14]. The details are given in Simovic et al. [15]. The two-fluid model, with these drag coefficient correlations, was used to model boiling flows in horizontal steam generators and kettle reboilers.

The aim of this study is to investigate the reliability of modelling methods for kettle reboilers in reproducing one-dimensional flow data. This is accomplished by obtaining two-phase pressure-drop data from a test bundle and comparing these, and other data, with predictions from the two-fluid model and the one-dimensional model implemented with three different void fraction correlations.

2 The two-fluid model

A one-dimensional version of the two-fluid model, similar to that used by Simovic et al. [15], was derived for adiabatic, steady state, fully developed flow. Thus, the conservation equations for energy were omitted and the mass equations reduced a constant velocity for each phase. The model was developed using the porous media approach, which assumes that the volume of the domain consists of a solid fraction, ε_s , a liquid fraction, ε_l , and a gas fraction, ε_g , so that the total volume fraction is

$$\varepsilon_s + \varepsilon_l + \varepsilon_g = 1 \quad (1)$$

The volume fraction available for flow, i.e. the porosity, ϕ , is

$$\phi = \varepsilon_g + \varepsilon_l = 1 - \varepsilon_s \quad (2)$$

For the square in-line tube bundles considered in this study, the porosity can be obtained from

$$\phi = 1 - \frac{\pi \left(\frac{D}{P}\right)^2}{4} \quad (3)$$

where D is the tube diameter and P is the tube pitch. The volume fraction of the gas and liquid phases are given by

$$\alpha_g = \frac{\varepsilon_g}{\phi} \quad \text{and} \quad \alpha_l = \frac{\varepsilon_l}{\phi} \quad (4, 5)$$

The momentum equation for the liquid phase can be written as

$$\varepsilon_l \frac{\partial p}{\partial y} = -\varepsilon_l \rho_l g + F_{gl} + F_{sl} \quad (6)$$

where F_{gl} is the force on the liquid by the gas per unit volume of domain and F_{sl} is the force on the liquid by the solid per unit volume of domain. The momentum equation for the gas phase is given by

$$\varepsilon_g \frac{\partial p}{\partial y} = -\varepsilon_g \rho_g g + F_{lg} + F_{sg} \quad (7)$$

where F_{lg} is the force on gas by the liquid per unit volume of domain and F_{sg} is the force on the gas by the solid per unit volume of domain. Equating pressure gradients from equations (6) and (7), with

$$F_{gl} = -F_{lg}, \text{ gives}$$

$$\alpha_g \phi (\rho_l - \rho_g) g - \left(1 + \frac{\alpha_g}{(1 - \alpha_g)}\right) F_{gl} + \frac{\alpha_g}{(1 - \alpha_g)} F_{sl} - F_{sg} = 0 \quad (8)$$

The force on the liquid by the gas per unit volume, F_{gl} , is related to the gas velocity u_g and the liquid velocity u_l through

$$F_{gl} = \frac{1}{2} C_D \rho_l A_{gl} (u_g - u_l) |u_g - u_l| \quad (9)$$

where C_D is the drag coefficient and the area of the gas bubbles, A_{gl} , is the cross sectional area of all N bubbles of diameter D_p that occupy a unit volume of domain. Thus

$$\varepsilon_g = N \frac{\pi D_p^3}{6} \quad (10)$$

so that

$$F_{gl} = \frac{3}{4} \phi \rho_l \alpha_g \frac{C_D}{D_p} (u_g - u_l) |u_g - u_l| \quad (11)$$

To close the model, the force on the gas by the tubes, F_{sg} , the force on the liquid by the tubes, F_{sl} , and the drag coefficient must be specified. For bubbly flow, the drag coefficient is obtained from the correlation of Ishii and Zuber [16], as adapted by Stevanovic et al. [11], i.e.

$$C_D = 0.267 D_p \left(\frac{g \Delta \rho}{\sigma} \right)^{0.5} \left(\frac{1 + 17.67(1 - \varepsilon)^{9/7}}{18.67(1 - \varepsilon)^{3/2}} \right)^2 \quad (12)$$

For churn flow, the equation proposed by Stevanovic et al. [11] is used, i.e.

$$C_D = 1.487 D_p \left(\frac{g \Delta \rho}{\sigma} \right)^{0.5} (1 - \varepsilon)^3 (1 - 0.75 \varepsilon)^2 \quad (13)$$

The force per unit volume on the liquid and on the gas by the solid are calculated respectively from

$$F_{sl} = \frac{f_l}{2} \rho_l j_l^2 (1 - \alpha_g) \quad (14)$$

and

$$F_{gl} = \frac{f_g}{2} \rho_g j_g^2 \alpha_g \quad (15)$$

where $f_i = \frac{k_i}{D}$, in which k_i ($i = l, g$) is the single-phase loss coefficients obtained from ESDU [17] and

D is the tube diameter. The single-phase loss coefficient is a function of Reynolds number based on the minimum superficial velocity, given for the liquid phase by

$$j_l = \frac{(1 - x) G_{\min}}{\rho_l (1 - \alpha_g)} \quad (16)$$

And for the gas phase by

$$j_g = \frac{xG_{\min}}{\rho_g \alpha_g} \quad (17)$$

in which x is the gas mass fraction. It should be noted that the porosity is not mentioned in equations 14 or 15 because it is included implicitly in the single-phase loss coefficient correlation.

3 The one-dimensional model

For a fully-developed flow, the momentum equation for the one-dimensional model is given by

$$\frac{\partial p}{\partial y} = -\rho_{tp} g + F_{sf} \quad (18)$$

where ρ_{tp} is the two-phase density, given by

$$\rho_{tp} = \alpha_g \rho_g + \alpha_l \rho_l \quad (19)$$

and F_{sf} is the force on the fluid by the tubes and is given by

$$F_{sf} = \frac{f_l}{2} \rho_l j_{lo}^2 \phi_l^2 \quad (20)$$

where j_{lo} is the liquid velocity when it flows alone and ϕ_l^2 is the two-phase multiplier, given by

$$\phi_l^2 = 1 + \frac{8}{X_{tt}} + \frac{1}{X_{tt}^2} \quad (21)$$

[18], in which X_{tt} is the Martinelli parameter, given by

$$X_{tt} = \left(\frac{1-x}{x} \right)^{0.9} \left(\frac{\rho_g}{\rho_l} \right)^{0.5} \left(\frac{\mu_l}{\mu_g} \right)^{0.1} \quad (22)$$

4 Experimental apparatus and procedure

In the present work, an in-line tube bundle has been designed and constructed to obtain pressure-drop data for air-water flows. The flow loop and the corresponding test section are illustrated in figures 2 and 3 respectively. Compressed air was supplied to the test section and was measured and adjusted using magnetically-coupled rotameters and manual valves. Three flow meters with ranges of 0-0.0039, 0-0.034

and 0-0.35 kg/s were used in a parallel arrangement. The accuracy of the flow meters was $\pm 1.6\%$. Water from the supply tank was measured using one of four different orifice plates, placed in parallel, downstream of the positive displacement pump. These were accurate to $\pm 1\%$. The water flow from the pump could pass to the test section or be returned to the supply tank through the re-circulation line. Adjustment of the manual valve placed in the re-circulation line gave the required water flow rate.

The test section consisted of five separable sections including a bubble generator, a convergent section, a settling length, the tube bundle and a second converging section, as shown in figure 3. These parts were fabricated from Perspex sheet 12 mm thick and joined together by bolts to provide a transparent view of the flow.

The bubble generator consisted of two pieces of porous tube 110 mm long and 50.0 mm in outside diameter placed in a rectangular Perspex box 224 mm in height \times 100 mm in depth \times 100 mm in width. The porous tube was manufactured by GKN Sinter Metals and had a small effective pore size of 206 microns (SIKA-B). Water entered the Perspex box from below. The air was fed to the porous tubes from both sides to produce a reasonably even two-phase flow that passed through the first convergent section and the 224 mm settling length before entering the tube bundle.

The tube bundle consisted of ten rows of tubes 38.0 mm in outside diameter with one full central column of tubes and two columns of half tubes placed on the walls to reduce bypass leakage. The tubes were 50 mm in length and were arranged in an in-line configuration with a pitch to diameter ratio of 1.32. The flow from the tube bundle passed through the second convergent section and into an air-water separator, where the air was released to the atmosphere and the water was returned to the supply tank.

Eleven pressure taps were placed across the rows to allow pressure drops across each tube to be measured. However, in this study, only the two-phase pressure drops between pressure taps 3 through to 10 are reported. The first two tubes and the last tube were excluded to avoid entrance and exit effects. The pressure drops were measured using a smart pressure transducer so that the pressure drop range could be adjusted. The upper range value was set to accommodate the expected pressure drop and thus

maximize the measurement accuracy. The pressure drop data were collected through a data logger connected to a PC controlled by Labview software. Before pressure drop readings were taken, all lines in the pressure-drop measurement system were purged with water to remove any air. The two-phase pressure drop measurements were conducted at approximately atmospheric pressure with $0.00047 < x < 0.57$ and $25 \leq G \leq 688 \text{ kg/m}^2\text{s}$. Each experiment was repeated to ensure repeatability. The pressure transducer was accurate to $\pm 0.25\%$

5 Model comparisons

5.1 Single Phase Pressure Drop

To test the experimental approach, air tests were undertaken at Reynolds numbers of 8920 and 19400.

The loss coefficient for each row was determined from

$$f = \frac{2\Delta P}{\rho u^2} \quad (23)$$

where ΔP is the pressure drop across each row, ρ is the density of the air, calculated from the ideal gas law with the absolute pressure taken from the first pressure tap, and u is the air velocity based on the largest flow area. The measured loss coefficients are compared with the correlation of ESDU [17] in figure 4. The figure reveals very large loss coefficients on the first row followed by increasing coefficients to about row 4, with constant values thereafter, indicating that fully developed flow exists from about row 4 onwards. The ESDU correlation agrees reasonably well with the measured fully-developed flow values. This indicates that the approach produces data comparable with previous researchers and justifies the use of the ESDU correlation for finding values to the single-phase loss coefficient used in the one-dimensional and two-fluid flow models.

5.2 Two-phase air-water pressure drop

The measured pressure drops were compared with predictions from the two-fluid model and the one-dimensional model. The one-dimensional model was used with three different void fraction correlations: Schrage et al. [1], Dowlati et al. [2] and Feenstra et al. [3]. The two-phase friction multiplier was obtained from Ishihara et al. [18], with the single-phase loss coefficient found from ESDU [17].

The Schrage correlation is given by

$$\alpha = \alpha_h (1 + 0.123 Fr^{-0.191} \ln x) \quad (24)$$

where the Froud number, Fr , is given by

$$Fr = \frac{G_{\max}}{\rho_l \sqrt{gD}} \quad (25)$$

and the homogeneous void fraction, α_h , is given by

$$\alpha_h = \frac{x}{\rho_g} + \frac{(1-x)}{\rho_l} \quad (26)$$

The Dowlati correlation is given by

$$\alpha = 1 - \frac{1}{(1 + C_1 j_g^* + C_2 j_g^{*2})^{1/2}} \quad (27)$$

where

$$j_g^* = \frac{\rho_g^{1/2} j_g}{\sqrt{gD(\rho_l - \rho_g)}} \quad (28)$$

and C_1 and C_2 depend on the fluid and the geometry of the tube bundle. For these data $C_1 = 30$ and $C_2 = 50$ were used, Dowlati et al. [14].

The Feenstra et al. [3] correlation is given by

$$\alpha = \left(1 + S \frac{\rho_g}{\rho_l} \left(\frac{1}{x} - 1 \right) \right)^{-1} \quad (29)$$

where the slip ratio, S , is given by

$$S = 1 + 25.7 (Ri \times Cap)^{0.5} (P/D)^{-1} \quad (30)$$

with the Richardson number, Ri , and the Capillary number, Cap , are calculated from

$$Ri = \Delta\rho^2 g(P-D) / G_{\max}^2 \quad \text{and} \quad Cap = \frac{\mu_l \mu_g}{\sigma} \quad (31, 32)$$

respectively, with the gas-phase velocity determined from

$$u_g = \frac{xG_{\max}}{\alpha\rho_g} \quad (33)$$

Figures 5-8 show the predicted pressure drops divided by the measured values varying with the gas mass fraction, or quality. The two-fluid model, figure 5, is shown to predict the pressure drop data to within $\pm 20\%$ if the mass flux lies between 312 and 688 kg/m²s. However, for mass fluxes out-with this range, the predictions are poor, particularly for gas mass fractions above 1%. The one-dimensional model, with the void fractions obtained from the Feenstra et al. [3] correlation, figure 6, or the Dowlati et al. [2], figure 7, predicts the measured data reasonably well for most mass fluxes. However, for the lower mass fluxes the predictions are less reliable. In contrast, the one-dimensional model with the Schrage et al. [1] correlation, figure 8, over-predicts most of the data for mass fluxes between 156 and 688 kg/m²s and is particularly poor for gas mass fractions above 2%.

5.3 Air-water data of Dowlati

Void-fraction and pressure-drop data were obtained by Dowlati et al. [2]. The experiments were performed in an in-line tube bundle with 20 rows and 5 columns of tubes with an outside diameter of 19 mm on a pitch to diameter ratio of 1.3. The experimental pressure drops presented were obtained from the single-phase frictional pressure drops, calculated from the correlation of Zukauskas [19], and the experimental two-phase multipliers. Figures 9 and 10 show a comparison of void fraction and pressure drop data for a range of gas mass fractions at mass fluxes of 96 and 503 kg/m²s with predictions from the two-fluid model and the one-dimensional model with the Feenstra et al [3] correlation, figure 9. The two-fluid and the one-dimensional model with the Feenstra et al. [3] correlation predict the void fraction data very well. However, the pressure drop results, figure 10, reveal that both models predict the pressure drop at a mass flux of 503 kg/m²s reasonably well but at the mass flux of 96 kg/m²s, both models significantly under predicts the data.

5.4 R113 vapour-liquid data of Dowlati

Experimental data obtained with R113 as the working fluid were reported by Dowlati et al. [20]. The experiments were carried out on an in-line tube bundle consisting of five columns and twenty rows of tubes, 12.7 mm in outside diameter on a 1.3 pitch to diameter ratio. The working fluid was boiled by feeding heated oil inside the tubes to generate uniform heating on all tubes. Figures 11 and 12 show the comparison of the two-fluid model predictions with the void fraction measurements at three different mass fluxes and a range of gas mass fractions. Also included in the figures are the predictions of the one-dimensional model with the correlations of Feenstra et al. [3] and Dowlati et al. [2]. For these predictions $C_1 = 10$ and $C_2 = 1$ were used, Dowlati et al. [20]. The two-fluid model does not predict the measured void fraction data very well, particularly at low mass flux, figure 11. It over predicts the experimental data over the range of mass fluxes by an average of 20%. The one-dimensional model with the correlation of Dowlati et al. [2] under predicts the data at low mass flux and over predicts it at higher values. The one-dimensional model with the correlation of Feenstra et al. [3] shows reasonable agreement with the measured data.

Dowlati et al. [20] reported that the two-phase friction multiplier correlation suggested by Ishihara et al. [18], predicted their experimental friction pressure drop data reasonably well for mass fluxes greater than $100 \text{ kg/m}^2 \text{ s}$. The two-fluid model is compared to this in figure 13 for a range of gas mass fractions. The two-fluid model substantially under-predicts the data at low gas mass fraction and over-predicts it at higher values.

6. Discussion

The predictions from the two-fluid model with the interfacial gas-liquid drag coefficient determined from the correlations proposed by Stevanovic et al. [11] have been compared to several experimental data sets. The comparison with the pressure-drop measurements from this study is poor, figure 5. The air-water void fraction data of Dowlati et al. [2] is predicted very well, figure 9. This is not surprising since these were part of the data set used in the formulation of the drag coefficient correlations. At first sight, the failure of the model to predict the corresponding pressure drop data is surprising, figure 10. However, the drag coefficient data were deduced by Simovic et al. [15] from equations 8 and 11, with the forces on the fluid by the tubes, F_{st} and F_{sg} , determined similarly to the method given in Section 2. Thus, the

experimental pressure drops were not used in the formulation of the drag coefficient correlations. The poor agreement in figures 5 and 10 is therefore indicative that the modelling of these forces does not capture the actual pressure drop characteristics. The drag coefficient correlations were deduced using only air-water data. The failure to predict the R113 void fraction data of Dowlati et al. [20], figures 11 and 12, suggests that the scaling parameters used in the formulation of the drag coefficient correlations may not allow them to be extrapolated to other fluids. Further work is needed to understand the forces on the fluid by the tubes so that more general drag coefficient correlations can be produced.

For most mass fluxes, the one-dimensional model compares reasonably well with the pressure drop data from the present study provided either the Dowlati et al. [2] or the Feenstra et al. [3] correlation is used to determine the void fraction, and the two-phase friction multiplier suggested by Ishihara et al. [18] is used to predict the frictional pressure drop, figures 6 and 7. The deviation at lower mass fluxes probably results from failings in the correlation for the two-phase friction multiplier, which has been reported to be inaccurate at these conditions, Dowlati et al. [2,14,20]. The failure of the model to predict the pressure drop data of Dowlati et al. [2], figure 10, is again indicative of the failings of the frictional pressure drop method at low mass fluxes. Dowlati et al. [2] reported that equation 21 predicted the experimental friction pressure drop data at mass fluxes above $260 \text{ kg/m}^2\text{s}$. Below this, the model under predicted the data. The poorer agreement between the R113 void fraction data of Dowlati et al. [20] and the correlation of Dowlati et al. [2] suggests that it is not as effective for a range of fluids as the correlation of Feenstra et al. [3]. The over-prediction in pressure drop by the one-dimensional model when the Schrage correlation is used to predict the void fraction, figure 8, is indicative of the failure of this method to predict air-water void fractions. Dowlati et al. [2] found that the Schrage et al. [1] correlation underestimated their void fraction measurements by up to 50%. Feenstra et al. [3] found that their model agreed very well with data from several investigators, except that of Schrage et al. [1]. Consequently, the higher pressure-drop predictions observed in figure 8 are probably caused by this void fraction correlation giving a higher gravity pressure drop than actually occurred. The under-predictions are again due to the low mass flux shortcomings of the frictional pressure drop method. Further work is therefore required to investigate the frictional pressure drop at low mass fluxes.

Most of the experiments reported are for controlled forced convection flows. In a kettle reboiler, the recirculation results from density differences between the in-bundle flow and the liquid flow between the bundle and the shell wall. These flows are one-dimensional at heat fluxes below 10 kW/m^2 , Burnside et al [6]. To show the consequences of the modelling approaches, a 17 tube column bundle of tubes, 19 mm in diameter on a 25 mm square pitch array was simulated to boil R113 at atmospheric pressure at a heat flux of 10 kW/m^2 . The pressure head was fixed as the hydrostatic head of liquid, which is a common design practice. A mass flux of $151 \text{ kg/m}^2\text{s}$ was predicted by the two-fluid model while $138 \text{ kg/m}^2\text{s}$ was predicted by the one-dimensional model using the Feenstra et al [3] correlation. This is not significantly different. However, the void fraction predictions are compared in figure 14, where the two-fluid model is shown to significantly over-predict the void fraction.

7. Conclusions

This study has investigated the modelling of one-dimensional data with one-dimensional methods. Of those investigated, the most accurate modelling method is the one-dimensional model with the Feenstra et al. [3] correlation used to find the void fraction and the Ishihara correlation [18] used to determine the two-phase multiplier and this is the best design method for kettle reboilers at low heat fluxes, less than 10 kW/m^2 . However, kettle reboilers at higher heat fluxes have a two-dimensional flow field, Burnside et al. [6]. Further work is therefore required to extend the one-dimensional models to two-dimensions. These methods should reduce to the one-dimensional flow model at low heat flux and therefore could be based on some form of extrapolation of them.

8. Nomenclature

A_p	Cross sectional area of the bubble	S	Slip ratio
Cap	Capillary number	u	Velocity
C_D	Drag coefficient	x	Quality
D	Tube diameter	X_{tt}	Martinelli parameter
D_p	Bubble diameter	Greek	

Fr	Froude number	ϕ	Porosity
F_{gl}	Force on the liquid by the gas per unit volume	ρ	Density
F_{sl}	Force on liquid by the solid per unit volume	ε	Volume fraction
F_{sg}	Force on the gas by the solid per unit volume	α	Void fraction
G	Mass flux	σ	Surface tension
g	Gravity acceleration	ϕ_1^2	Two phase friction multiplier
j	Superficial velocity	μ	Viscosity
j_g^*	Dimensionless gas velocity	Subscripts	
k	Single loss coefficient	l	Liquid
N	Number of bubbles	g	Gas
P	Tube pitch	$_{min}$	Minimum
Q	Volume liquid flow rate	$_{max}$	maximum

8. References

- [1]. Schrage, D. S., Hsu, J. T. and Jensen, M. K., 1988, Two-Phase Pressure Drop in Vertical Crossflow across a Horizontal Tube Bundle, *AIChE Journal*, Vol. 34(1), pp. 107-115.
- [2]. Dowlati, R., Kawaji, M. and Chan, A. M. C., 1990, Pitch-to-Diameter Effect on Two-Phase Flow across an in-Line Tube Bundle, *AIChE Journal*, Vol. 36(5), pp. 765-772.
- [3]. Feenstra, P. A., Weaver, D. S. and Judd, R. L., 2000, Improved Void Fraction Model for Two-Phase Cross-Flow in Horizontal Tube Bundles, *International Journal of Multiphase Flow*, Vol. 26(11), pp. 1851-1873.
- [4]. Lockhart, R. W. and Martinelli, R. C., 1949, Proposed Correlation of Data for Isothermal Two-Phase, Two-Component Flow in Pipes, *Chemical Engineering Progress*, Vol. 45(1), pp. 39-48.
- [5]. Chisholm, D. and Laird, A. D. K., 1958, Two-Phase Flow in Rough Tubes, *Trans. ASME*, Vol. 80(2), pp. 276-286.
- [6]. Burnside, B. M., Miller, K. M., McNeil, D. A. and Bruce, T., 2001a, Heat Transfer Coefficient Distributions in an Experimental Kettle Reboiler Thin Slice, *Chemical Engineering Research and Design*,

Vol. 79(4), pp. 445-452.7.

- [7]. Burnside, B. M., 1999, 2-D Kettle Reboiler Circulation Model, *International Journal of Heat and Fluid Flow*, Vol. 20(4), pp. 437-445.
- [8]. Edwards, D. P. and Jensen, M. K., 1991, Two-Dimensional Numerical Model of Two-Phase Heat Transfer and Fluid Flow in a Kettle Reboiler, *American Society of Mechanical Engineers, Heat Transfer Division, (Publication) HTD*, Minneapolis, MN, USA, Vol. 159, pp. 9-16
- [9]. Rahman, F. H., Gebbie, J. G. and Jensen, M. K., 1996, Interfacial Friction Correlation for Shell-Side Vertical Two-Phase Cross-Flow Past Horizontal in-Line and Staggered Tube Bundles, *International Journal of Multiphase Flow*, Vol. 22(4), pp. 753-766.
- [10]. Stosic, Z. V. and Stevanovic, V. D., 2002, Advanced Three-Dimensional Two-Fluid Porous Media Method for Transient Two-Phase Flow Thermal-Hydraulics in Complex Geometries, *Numerical Heat Transfer, Part B: Fundamentals*, Vol. 41(3-4), pp. 263-289.
- [11]. Stevanovic, V. D., Stosic, Z. V., Kiera, M. and Stoll, U., 2002a, Horizontal Steam Generator Thermal-Hydraulics at Various Steady-State Power Levels, *International Conference on Nuclear Engineering, Proceedings, ICONE*, Arlington, VA, United States, Vol. 3, pp. 767-779
- [12]. Stevanovic, V. D., Stosic, Z. V., Kiera, M. and Stoll, U., 2002b, Numerical Simulation and Analyses of the Loss of Feedwater Transient at the Unit 4 of Kola Npp, *International Conference on Nuclear Engineering, Proceedings, ICONE*, Arlington, VA, United States, Vol. 3, pp. 781-792
- [13]. Pezo, M., Stevanovic, V. D. and Stevanovic, Z., 2006, A Two-Dimensional Model of the Kettle Reboiler Shell Side Thermal-Hydraulics, *International Journal of Heat and Mass Transfer*, Vol. 49(7-8), pp. 1214-1224.
- [14]. Dowlati, R., Chan, A. M. C. and Kawaji, M., 1992a, Hydrodynamics of Two-Phase Flow across Horizontal in-Line and Staggered Rod Bundles, *Journal of Fluids Engineering, Transactions of the ASME*, Vol. 114(3), pp. 450-456.
- [15]. Simovic, Z. R., Ocokoljic, S. and Stevanovic, V. D., 2007, Interfacial Friction Correlations for the Two-Phase Flow across Tube Bundle, *International Journal of Multiphase Flow*, Vol. 33(2), pp. 217-226.
- [16]. Ishii, M. and Zuber, N., 1979, Drag Coefficient and Relative Velocity in Bubbly, Droplet or Particulate Flows, *AIChE Journal*, Vol. 25(5), pp. 843-855.
- [17]. ESDU, 1979, Crossflow Pressure Loss over Banks of Plain Tubes in Square and Triangular Arrays

Including Effects of Flow Direction, *Engineering Sciences Data Unit*, Vol.(79034), pp. 17.

[18]. Ishihara, K., Palen, J. W. and Taborek, J., 1980, Critical Review of Correlations for Predicting Two-Phase Flow Pressure Drop across Tube Banks, *Heat Transfer Engineering*, Vol. 1(3), pp. 23-32.

[19]. Zukauskas, A., 1972, Heat Transfer from Tubes in Crossflow (Heat Transfer and Hydraulic Resistance of Single Banks and Systems of Tubes in Cross Flow of Gases and Viscous Liquids), *Advances in heat transfer.*, Vol. 8, pp. 93-160.

[20]. Dowlati, R., Kawaji, M. and Chan, A. M. C., 1996, Two-Phase Crossflow and Boiling Heat Transfer in Horizontal Tube Bundles, *Journal of Heat Transfer, Transactions ASME*, Vol. 118(1), pp. 124-131.

Figure captions

Figure 1: typical kettle reboiler, Pezo et al., [13]

Figure 2: In-bundle flow loop

Figure 3: Test section

Figure 4: Variation of the air-only loss coefficient with row number

Figure 5: Variation of predicted to measured pressure drop with quality for the two-fluid model

Figure 6: Variation of predicted to measured pressure drop with quality for the one-dimensional model with the Feenstra correlation

Figure 7: Variation of predicted to measured pressure drop with quality for the one-dimensional model with the Dowlati correlation

Figure 8: Variation of predicted to measured pressure drop with quality for the one-dimensional model with the Shrage correlation

Figure 9: Variation of void fraction with quality

Figure 10: Variation of pressure drop with quality

Figure 11: Variation of void fraction with quality

Figure 12: Variation of void fraction with quality

Figure 13: Variation of two-phase frictional pressure drop with quality

Figure 14: Variation of void fraction with row number for a tube bundle boiling atmospheric R113 at 10 kW/m²

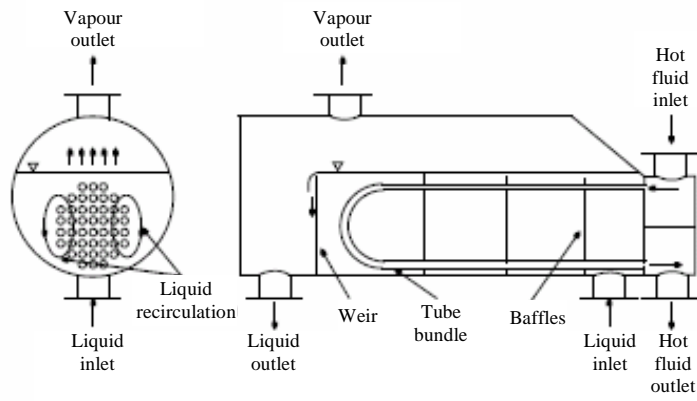


Figure 1: typical kettle reboiler, Pezo et al., [13]

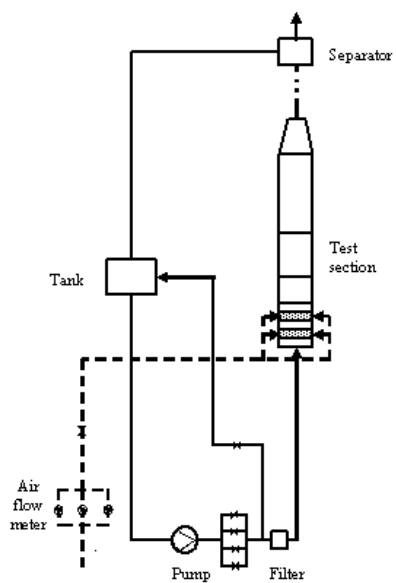


Figure 2: In-bundle flow loop

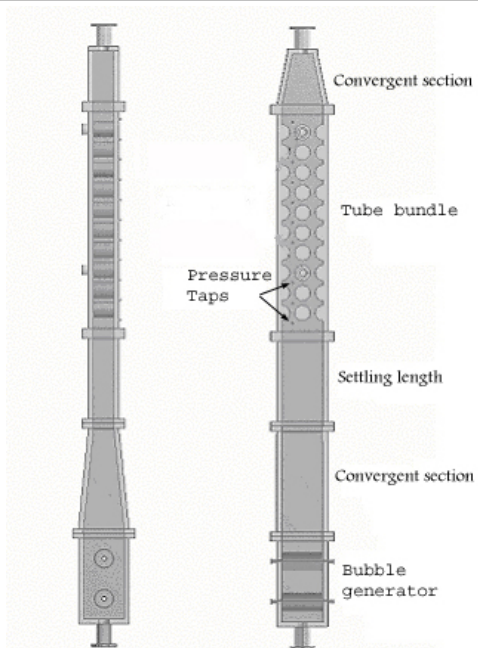


Figure 3: Test section

Figure 4: Variation of the air-only loss coefficient with row number

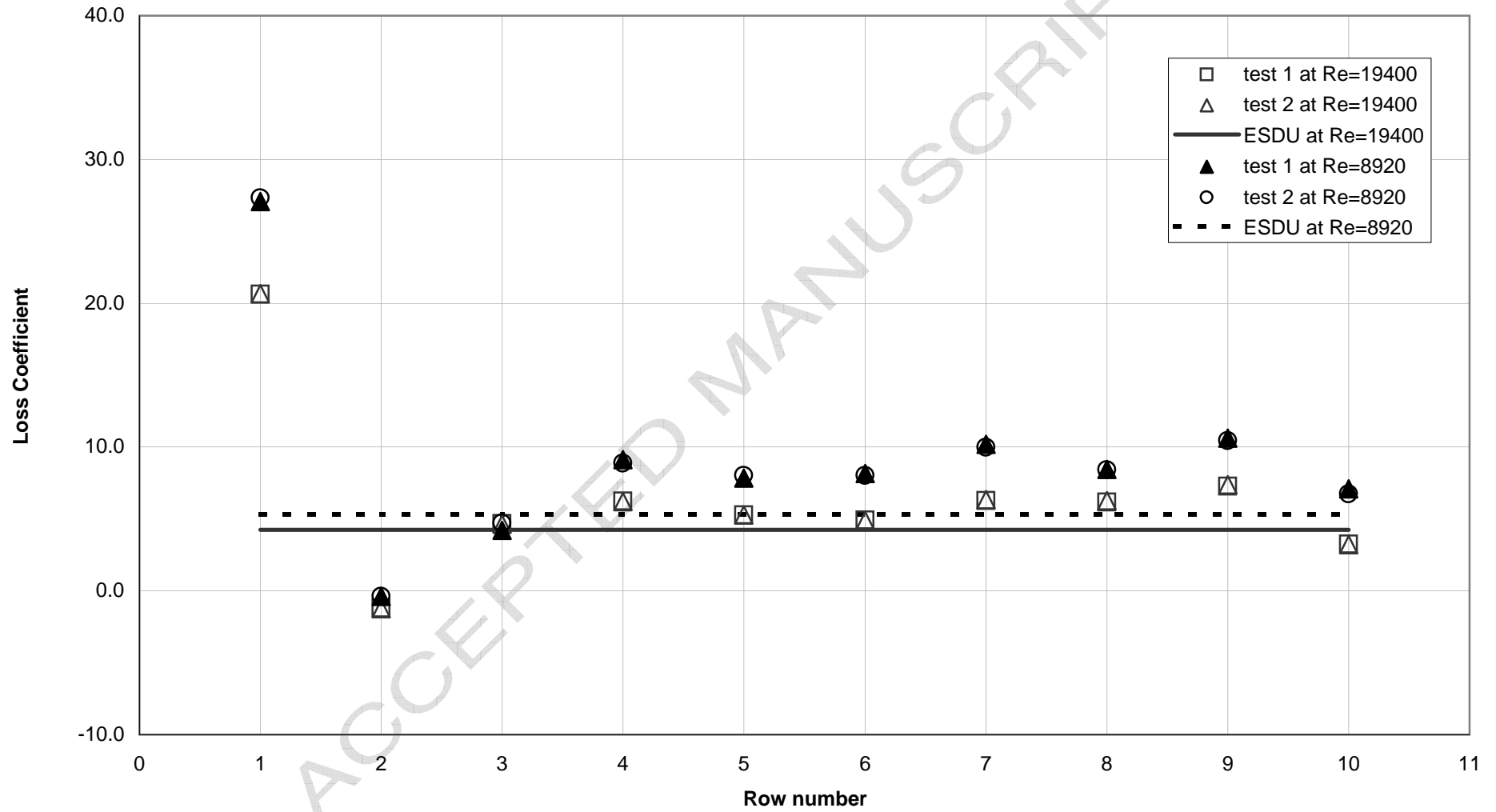


Figure 5: Variation of predicted to measured pressure drop with quality for the two-fluid model

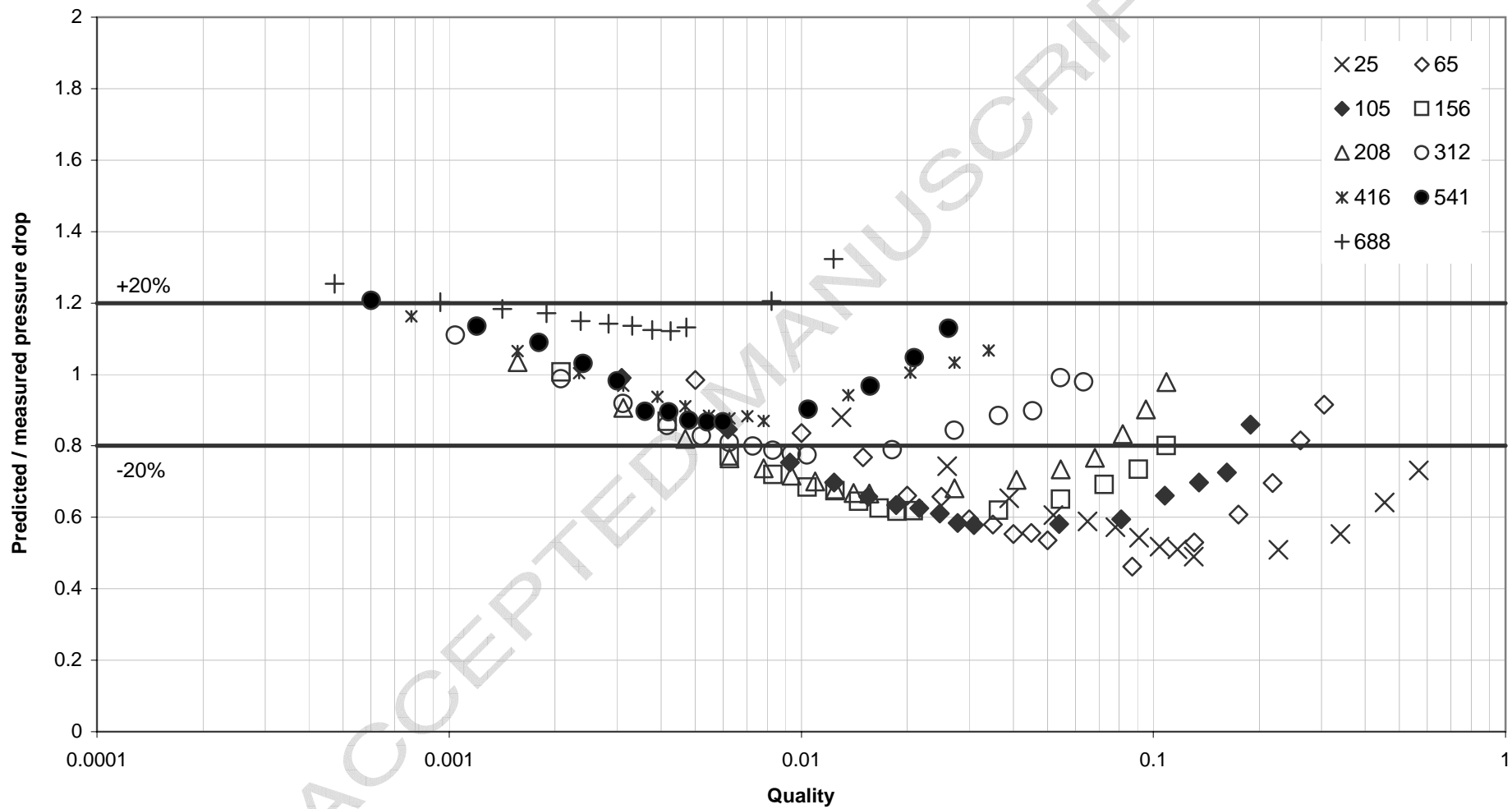


Figure 6: Variation of the predicted to measured pressure drop with quality for the one-dimensional model with the Feenst correlation

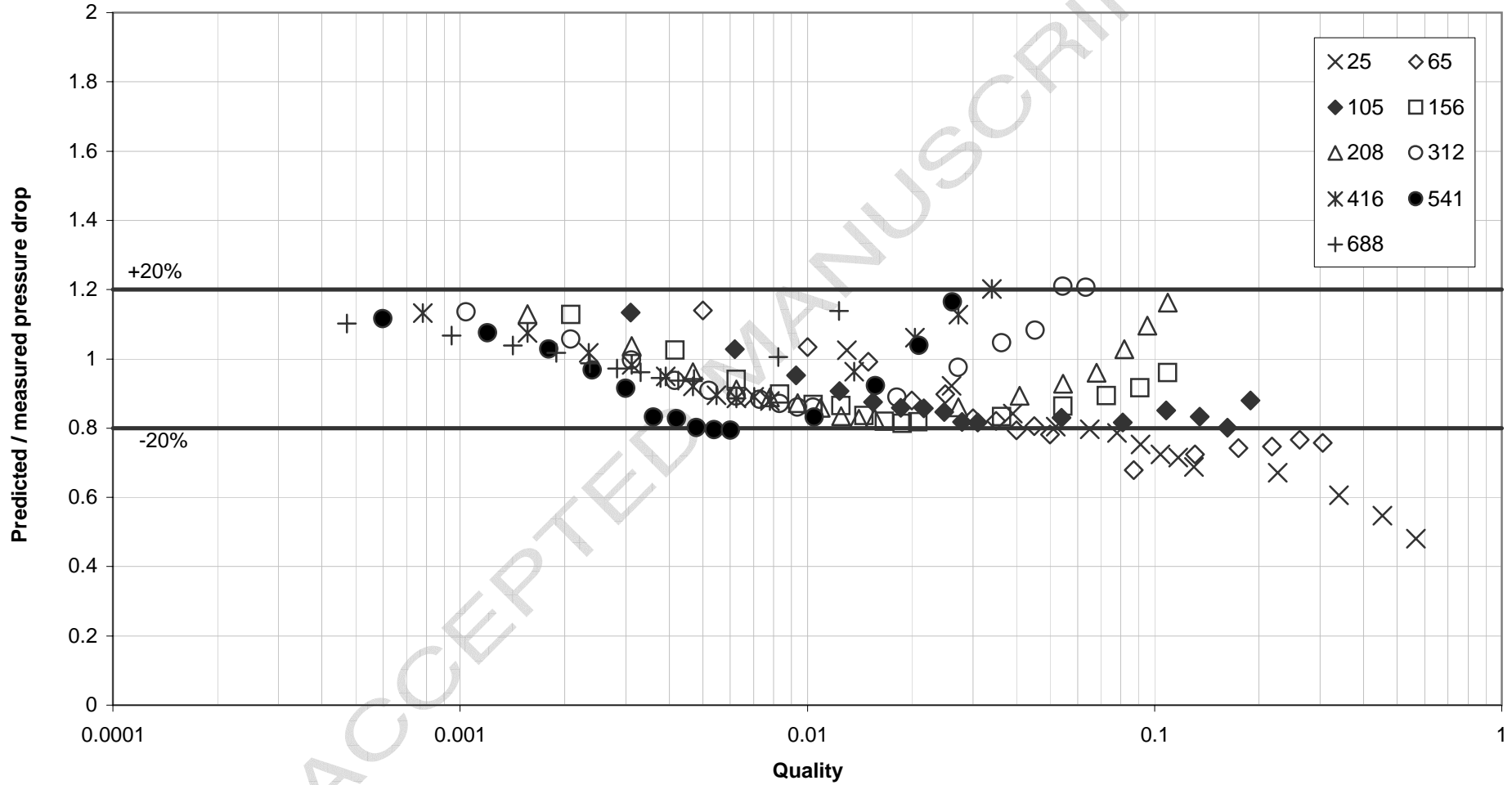


Figure 7: Variation of the predicted to measured pressure drop with quality for the one-dimensional model with the Dowlah correlation

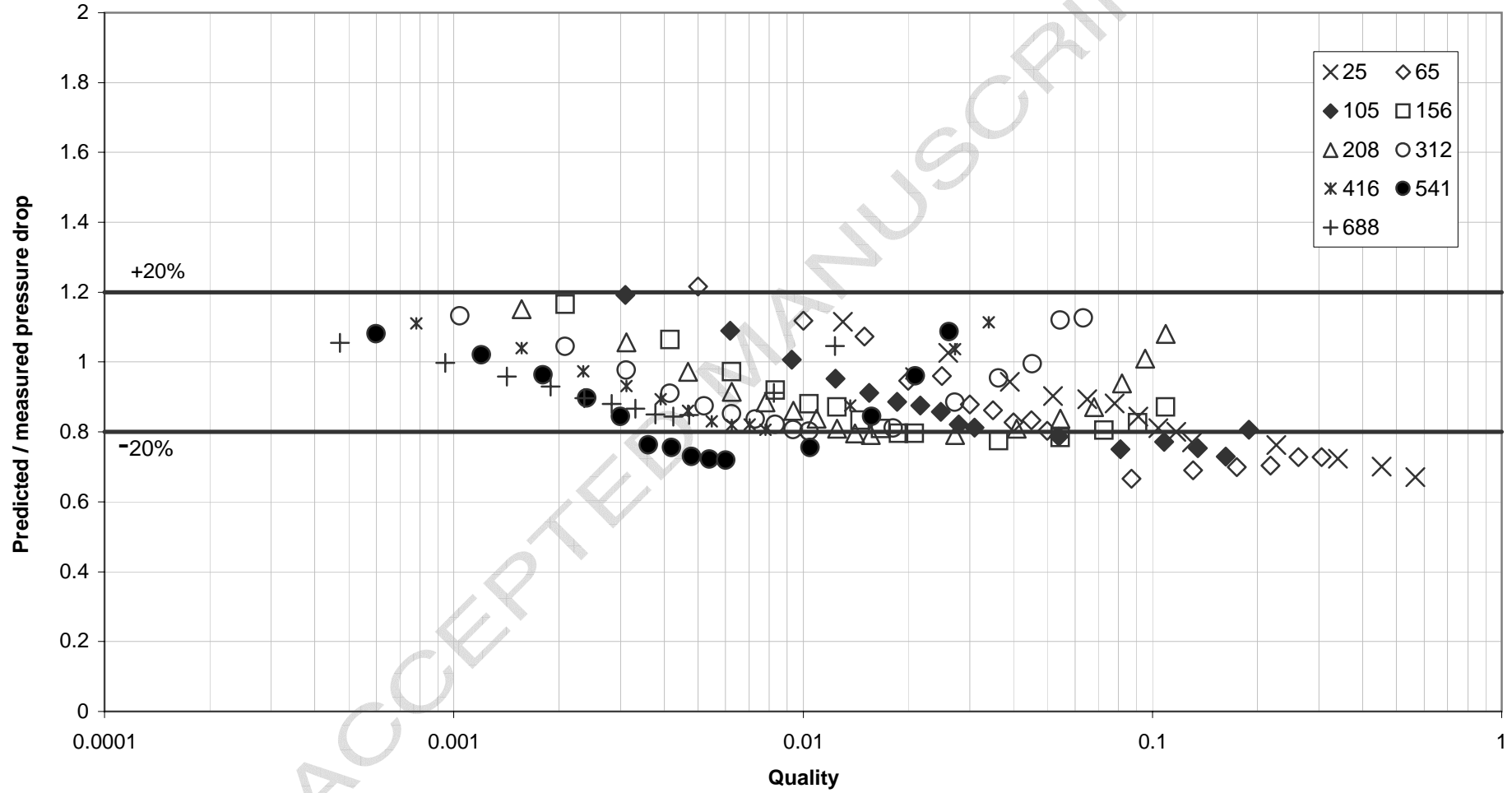


Figure 9: Variation of void fraction with quality

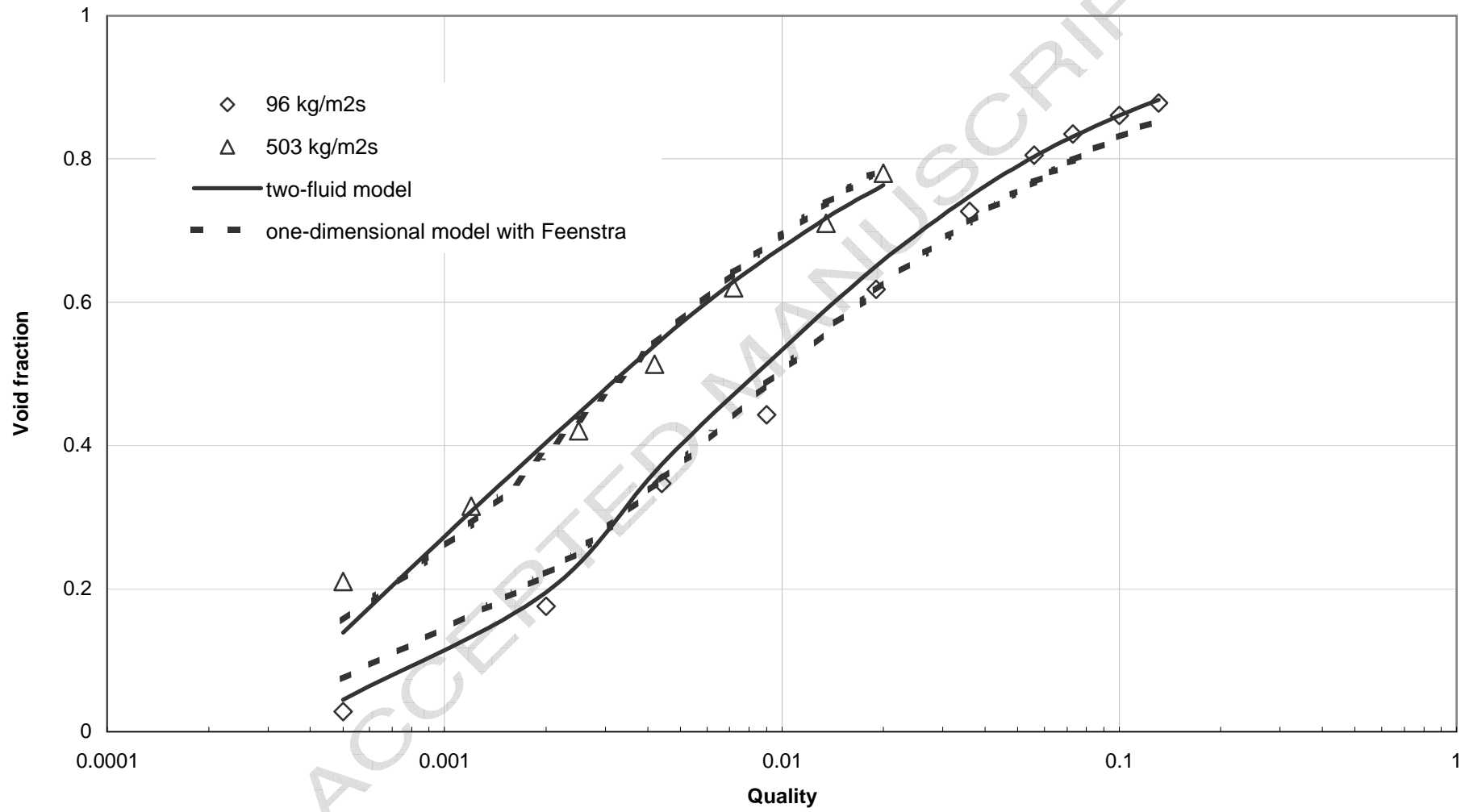


Figure 10: Variation of pressure drop with quality

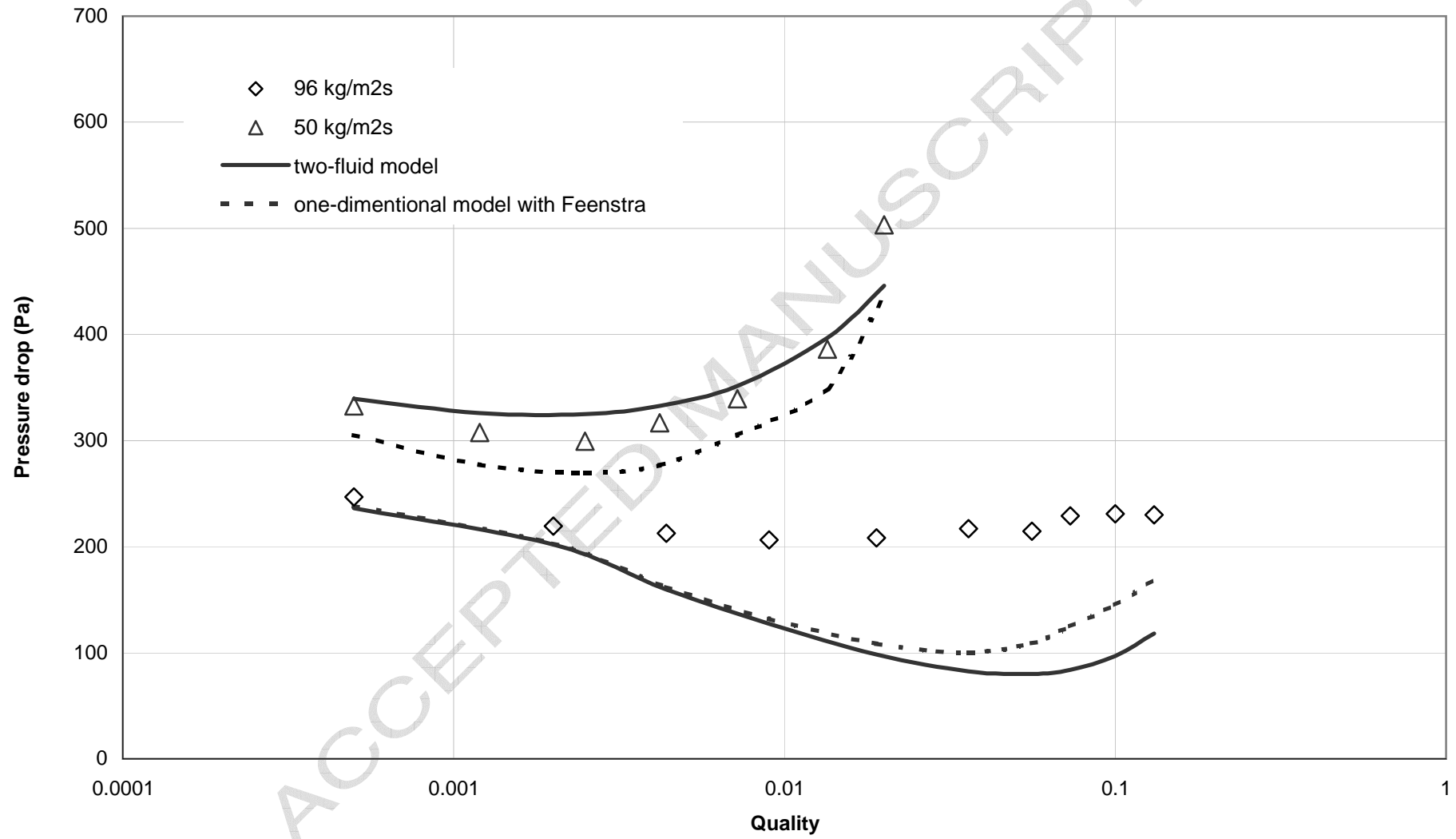


Figure 11: Variation of void fraction with quality

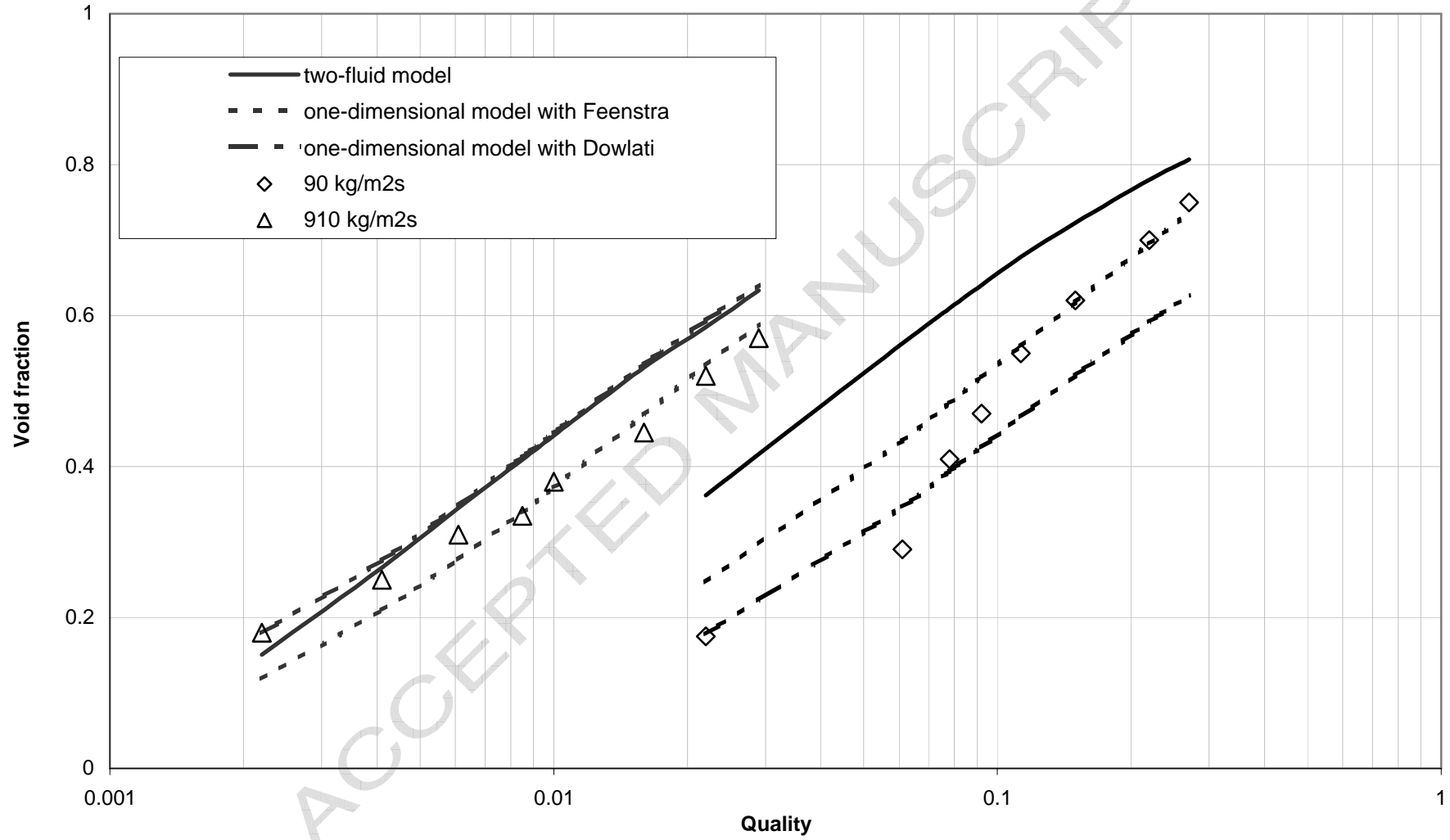


Figure 12: Variation of void fraction with quality

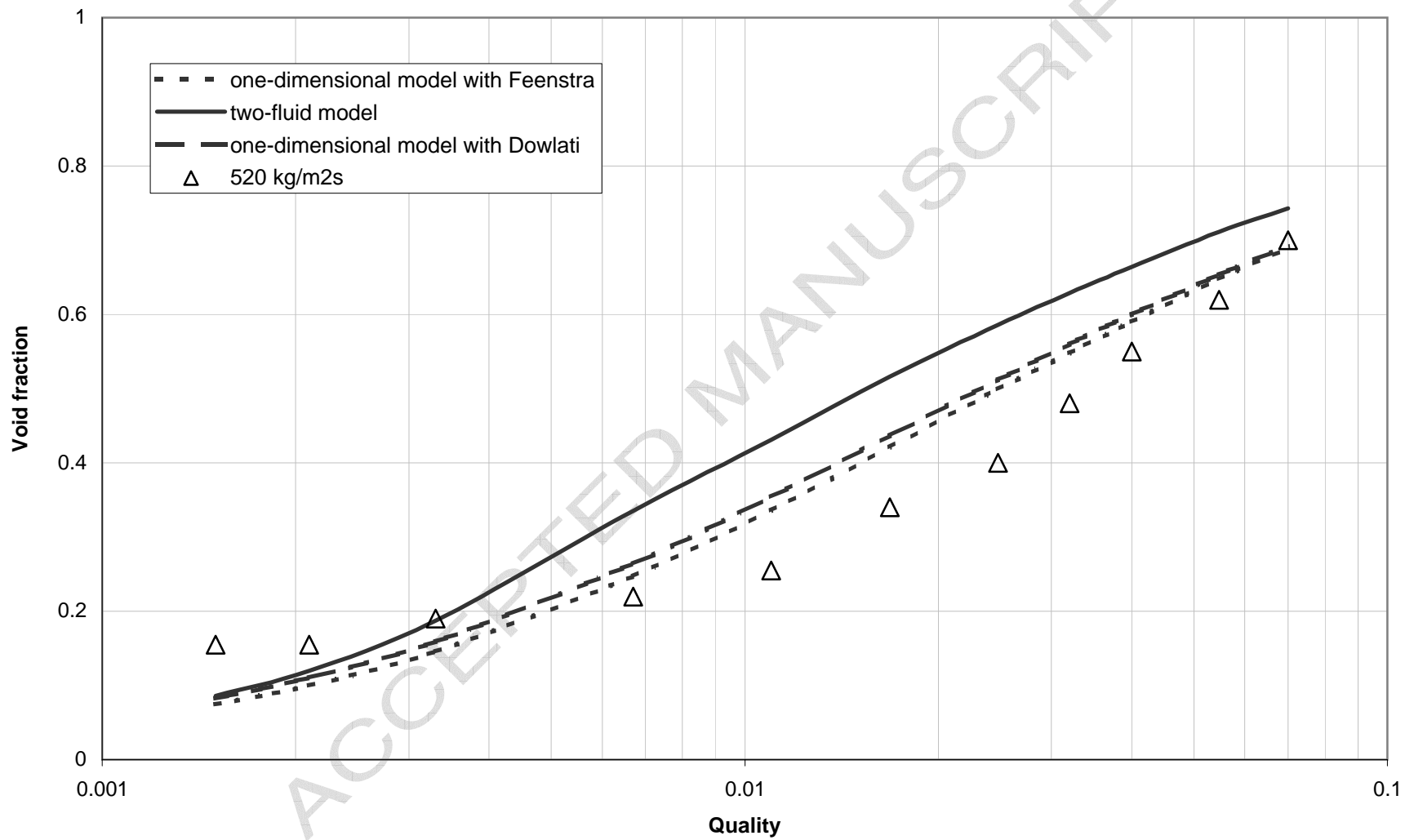


Figure 13: Variation of two-phase frictional pressure drop with quality

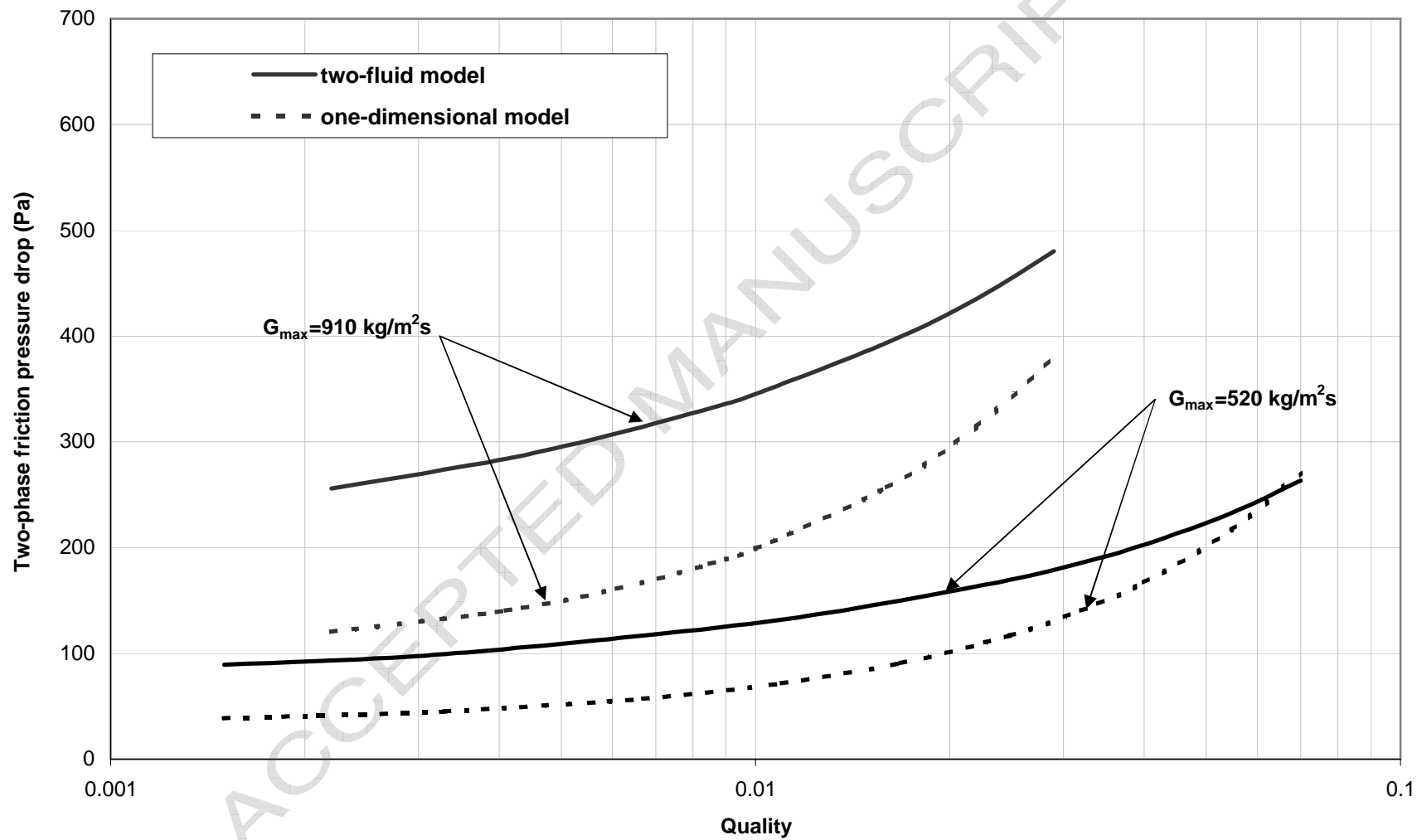


Figure 14: Variation of void fraction with row number for a tube bundle boiling atmospheric R113 at 10 kW/m^2

